

## Convergence analysis of full elastic tensors to homogenization predictions in periodic composite material design

**P.G. Coelho<sup>1</sup>, L.D. Amiano<sup>2</sup>, J.M. Guedes<sup>3</sup>, H.C. Rodrigues<sup>3</sup>**

<sup>1</sup> UNIDEMI, DEMI, Faculty of Sciences and Technology, Universidade Nova de Lisboa, Portugal, pgc@fct.unl.pt

<sup>2</sup> DEMI, Faculty of Sciences and Technology, Universidade Nova de Lisboa, Portugal

<sup>3</sup> IDMEC, Universidade de Lisboa, Portugal

### 1. Abstract

Periodic homogenization models are often used to compute the elastic properties of periodic composite materials based on the shape and periodicity of a given material microstructure. This paper extends previous work to 3-D analysis and anisotropic design cases investigating how rapidly the mean compliance and the 21 independent elastic coefficients from the apparent stiffness tensor converge to the corresponding values of the homogenized tensor. The outcome indicates that it is sufficient to have a low scale factor to replace the non-homogeneous composite by the equivalent homogeneous material with the moduli computed by homogenization.

**2. Keywords:** Homogenization, Optimization, Topology, Scale, Cellular

### 3. Introduction

The optimal design of periodic composites has been an area of intense research [1]. The so-called "unit-cell" is the microstructure representative of the smallest periodic heterogeneity of the material domain. The resulting macroscopic material is then defined assembling unit-cells. The use of continuum finite elements, homogenization and the SIMP (Solid Isotropic Material with Penalization) parameterization constitutes the traditional approach to obtain optimized porous materials through topology optimization. Topology optimization, in the frame of continuum elasticity, is an iterative design method that optimizes a material distribution in a given design domain with respect to a specified objective function and a set of constraints [2]. Topology optimization can be used to design materials by inverse homogenization. In this case the microstructure does not exist a priori but one seek to come up with a microstructure (interior topology of a unit-cell) using objective functions that consider prescribed or extreme homogenized properties [3].

In this work one uses the inverse homogenization method to extremize the energy density based objective function subjected to volume or permeability constraints. For instance, ensuring permeability isotropy while prescribing a preferential stiffness direction is of practical interest concerning bone implants (scaffolds). Bio-transport properties in the scaffold region is fundamental because cells, nutrients and waste products are supposedly to migrate easily inside the scaffold microstructure for tissue regeneration. At the same time the scaffold is a bearing load device which demands for increased mechanical stiffness. An appropriate trade-off between the conflicting properties of permeability and stiffness can be achieved by performing topology optimization [4-9].

The inverse homogenization method assumes that the scale of a unit-cell is indeterminate (infinitely small) as well as periodic Boundary Conditions (BC's) [10-13]. This makes uncertain whether the obtained topology can be translated into real composites of macroscale. In practice, one has a finite number of measurable unit-cells assembled together to define the composite material. Moreover, the stress or strain fields are in general arbitrary (not periodic) near the boundary of the composite.

Therefore one important contribution here is to investigate scale-size effects on the mechanical response of periodic materials with finite periodicity applying standard testing procedures and compare them with the predictions from the homogenization method. This study follows similar studies already reported in the literature which investigated scale-size effects although involving only two-dimensional bi-material unit-cells with prescribed material symmetry, see [14-17]. This work extends the analysis of the scale-size effects to solid-void three-dimensional periodic composites, anisotropic design cases and investigates how rapidly the mean compliance and the 21 independent elastic coefficients from the apparent fourth-order stiffness tensor converge to the corresponding values of the homogenized stiffness tensor.

### 4. Material model

The material model here is a 3-D porous composite material generated by the repetition of a unit-cell in all directions of the space. The unit-cell represents the smallest periodic heterogeneity of the composite domain  $\Psi$ . Periodic repetition of a unit-cell made up of a given parent material will yield a porous macroscopic material whose constitutive properties may differ substantially from the parent one. This macroscopic behavior can be

evaluated using homogenization theory. This theory assumes periodic boundary conditions (BC's) applied to the unit-cell domain  $Y$  and infinite periodicity of the unit-cell ( $Y$ -periodic), i.e. its feature size  $d$  is much smaller than the cellular material global size  $D$  ( $d/D \rightarrow 0$ ), see Fig. 1a. These assumptions make uncertain whether the obtained topology can be translated into real composites of macroscale. In practice, the composite material comprises a finite number of measurable unit-cells and the stress or strain fields are not periodic near the structure boundary. The optimal material microstructure topology is found here using the topology optimization method applied to the unit-cell design domain  $Y$ . This domain is considered cubic and unitary,  $|Y| = 1$ . For a numerical problem solution, this domain is discretized using 8-node isoparametric hexahedral finite elements such that the resulting mesh is  $20 \times 20 \times 20$  elements, see Fig. 1b. The effective material properties (homogenized properties) can be found using a numerical homogenization procedure described in [13]. The relative density  $\mu$  of material in each finite element is the problem design variable and it is assumed constant inside the element volume. Solid and void corresponds to  $\mu = 1$  and 0, respectively. The topology optimization problem may consist in finding the distribution of density  $\mu$  in  $Y$  that extremizes the elastic energy density given a stress field as detailed in the next section.

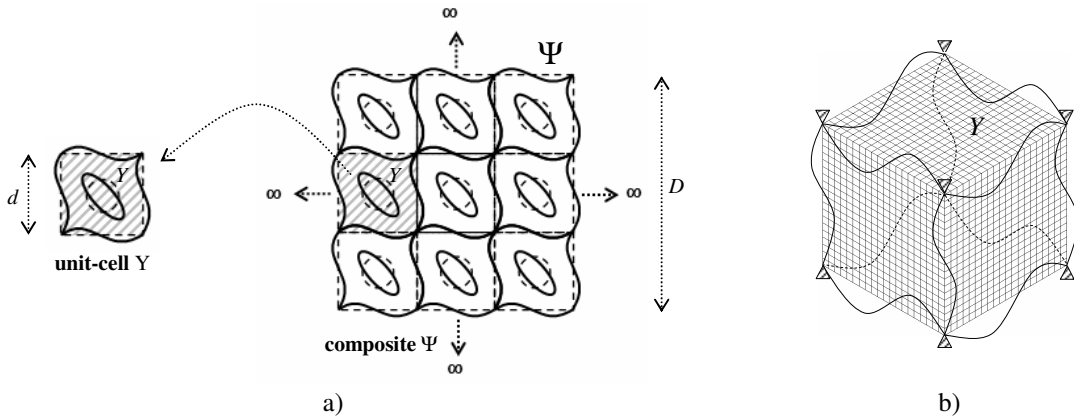


Figure 1: a) Material model to be interpreted in the light of the homogenization theory. Array of  $n \times n \times n$  unit-cells of global size  $D$  and one unit-cell of size  $d$ . Periodic boundary conditions are illustrated; b) Material numerical model with schematic periodic boundary conditions.

## 5. Optimization problem

The local anisotropy problem of finding the optimal lay-out of a unit-cell for minimum compliance and requiring at least orthotropic permeability or prescribed volume fraction can be stated as,

$$\begin{aligned} \min_{\mu} \frac{1}{2} C_{mnlk}^H(\mu) \bar{\sigma}_{mn} \bar{\sigma}_{kl} \\ K_{ij}^H(\mu) \geq k^* ; i=j=1, \dots, 3 \wedge K_{ij}^H(\mu) = 0 ; i \neq j \text{ and } i, j = 1, \dots, 3 \\ \text{or} \\ \int_Y \mu(\mathbf{y}) dY \leq V^* \end{aligned} \quad (1)$$

In Eq. (1)  $\mu$  is the local density varying between 0 (void) and 1 (material) which depends on the spatial variable  $\mathbf{y}$  in the unit-cell design domain  $Y$ . The stress tensor is  $\bar{\sigma}$  and characterizes an averaged macroscopic stress field applied to the composite. The homogenized compliance tensor is  $\mathbf{C}^H$ , i.e. the inverse of the homogenized stiffness tensor  $\mathbf{E}^H$ . The stiffness tensor at each point of  $Y$  is related to the tensor  $\mathbf{E}^0$  of the base material properties through the SIMP interpolation scheme [18]. Regarding the permeability constraints, one enforces the permeability tensor to be diagonal and each diagonal coefficient has to be "equal" or "greater than" a threshold,  $k^*$ . This way one gets an interconnected pore network on the periodic material satisfying a critical (minimum) permeability in all direction of the space. The permeability measure of porous media is given by the homogenized tensor  $\mathbf{K}^H$ . This tensor is obtained homogenizing a potential flow problem in periodical porous media characterized by the Darcy law (Darcy flow is assumed) [10,12]. Here one considers the interpolation between permeability and local density  $\mu$  given by a power-law (see e.g. [19,20]). The permeability tensor for the base material,  $\mathbf{K}^0$ , is here considered to be unitary, diagonal and isotropic. This way the interpolation scheme means that void and solid have high (100%) and low (0%) permeability, respectively. Consequently, the homogenized permeability tensor  $\mathbf{K}^H$  characterizing the periodic material medium becomes normalized, i.e. its coefficients take values between 0 and 1 (0% and

100%), and thus the threshold  $k^*$  in Eq. (1) can also be fixed between these bounds.

## 6. Numerical testing procedures

Recall that the homogenized elastic properties in Eq. (1) are calculated when  $n \rightarrow \infty$ . Consequently, they are  $n$  independent and there is no size of the unit-cell ( $d \rightarrow 0$ ). That is why, it is critical to investigate how accurate homogenization predictions are compared to the actual properties of a composite with the unit-cell scaled  $n$  times. In this work the scale factor  $n$ , defined as  $D/d$  with  $D = 1$ , varies from 1 to 6 as illustrated in Fig. 2.

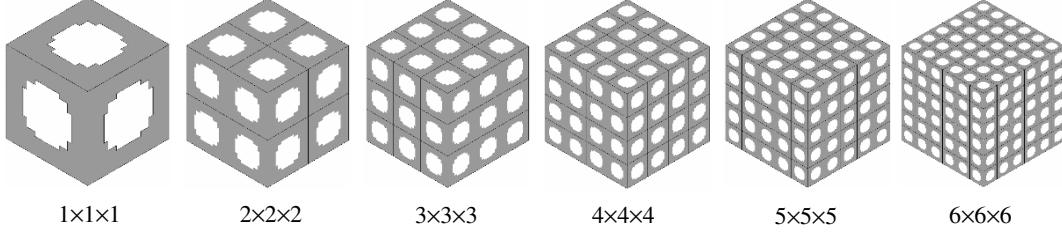


Figure 2: Unitary arrays containing  $n \times n \times n$  unit-cells ( $n$  varies from 1 to 6).

In order to estimate apparent elastic properties, this work follows a standard numerical testing procedure described in [21] and summarized as follows. For instance, let's consider the Dirichlet-type displacement boundary conditions,

$$\mathbf{u}(\mathbf{x})|_{\partial\Psi} = \Theta^{(i)} \cdot \mathbf{x}|_{\partial\Psi} \quad i = 1 \text{ to } 6 \quad (2)$$

as well as the Neumann-type traction boundary conditions:

$$\boldsymbol{\sigma}(\mathbf{x}) \cdot \mathbf{n}|_{\partial\Psi} = \Theta^{(i)} \cdot \mathbf{n}|_{\partial\Psi} \quad i = 1 \text{ to } 6 \quad (3)$$

where

$$\Theta^i = \begin{bmatrix} \beta & 0 & 0 \\ 0 & 0 & 0 \\ 0 & 0 & 0 \end{bmatrix}, \begin{bmatrix} 0 & 0 & 0 \\ 0 & \beta & 0 \\ 0 & 0 & 0 \end{bmatrix}, \begin{bmatrix} 0 & 0 & 0 \\ 0 & 0 & 0 \\ 0 & 0 & \beta \end{bmatrix}, \begin{bmatrix} 0 & \beta & 0 \\ \beta & 0 & 0 \\ 0 & 0 & 0 \end{bmatrix}, \begin{bmatrix} 0 & 0 & 0 \\ 0 & 0 & \beta \\ 0 & \beta & 0 \end{bmatrix}, \begin{bmatrix} 0 & 0 & \beta \\ 0 & 0 & 0 \\ \beta & 0 & 0 \end{bmatrix} \quad (4)$$

and  $\partial\Psi$  is the boundary of the composite sample  $\Psi$ ,  $\mathbf{u}$  is the displacement vector,  $\mathbf{x}$  is the spatial position vector,  $\boldsymbol{\sigma}$  is the Cauchy stress tensor,  $\mathbf{n}$  is the outward normal unit vector and  $\beta$  is a constant. The upper script index  $i$  on tensor  $\Theta$  means the application of six fundamental tests (three normal and three shear mechanical tests shown in Eq. 4). In the case of Dirichlet-type conditions, where the applied displacement field is  $x$  linearly dependent, the sample  $\Psi$  is tested at a uniform strain  $\beta$ . In case of Neumann's, the test is carried out on  $\Psi$  at a uniform stress  $\beta$ . The specific nature of the Dirichlet and Neumann-type conditions allow direct estimation of the stiffness and compliance tensors, referred to as Dirichlet  $\mathbf{E}^D$  and Neumann  $\mathbf{C}^N$  tensors, respectively. In both cases, average stress  $\langle \boldsymbol{\sigma} \rangle$  and strain  $\langle \boldsymbol{\varepsilon} \rangle$  fields are computed in the volume  $|\Psi|$  and then,

$$\langle \boldsymbol{\sigma} \rangle = \mathbf{E}^D \langle \boldsymbol{\varepsilon} \rangle \quad \text{and} \quad \langle \boldsymbol{\varepsilon} \rangle = \mathbf{C}^N \langle \boldsymbol{\sigma} \rangle \quad (5)$$

In turn, defining  $\mathbf{E}^N = (\mathbf{C}^N)^{-1}$  as the Neumann stiffness tensor, yields

$$\langle \boldsymbol{\sigma} \rangle = \mathbf{E}^N \langle \boldsymbol{\varepsilon} \rangle \quad (6)$$

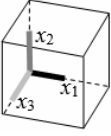
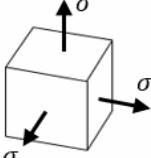
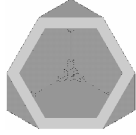
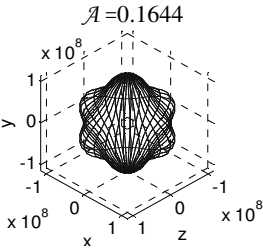
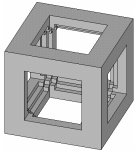
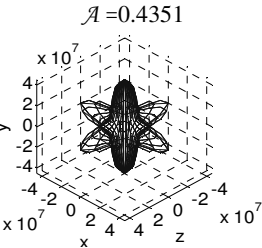
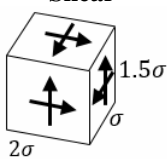
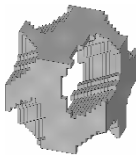
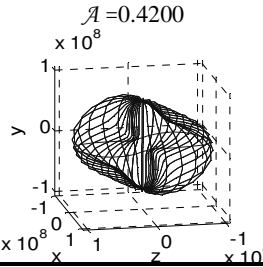
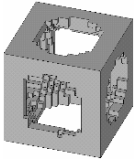
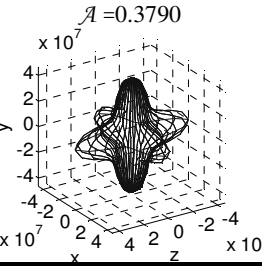
One considers here two additional types of BC's because Neumann-type conditions underestimate too much the apparent properties of porous materials due to the larger compliance of the void phase near the boundary.

On the one hand, one pursues a battery of fundamental tests applying the constant pressure, either normal or shear, only on the solid phase. On the other hand, one applies mixed BC's, i.e. a uniform pressure upon a rigid plate that in turn transfers the normal load to the top surface of the "solid" and "void" elements. Using rigid plates for shear tests here is cumbersome. For shear, one applies instead displacement-based BC's as given by Eq. (2),  $i = 4$  to 6. However, the displacements are only applied to two sets of opposite facets and only the displacements that are  $\mathbf{x}$ -dependent are applied (this is less restrictive than Dirichlet's). The application of these additional BC's is restricted here to orthotropic designs for the sake of getting tensor symmetry and static equilibrium.

## 7. Results

Two macroscopic stress fields are selected for demonstration purposes, *hydrostatic* and three different *shear* forces as indicated in Table 1. The corresponding optimal microstructures are shown considering either volume or permeability as design constraints in Eq. (1). The hydrostatic optimal solution with volume constraint is a closed-wall unit-cell (cut section view is shown) whereas the remaining cases show an open-cell microstructure as optimal. The anisotropy plots along with parameter  $\mathcal{A}$  shown in Table 1 are also used and explained in [22,23].

Table 1: Macroscopic stress fields and corresponding optimal designs (solid part only) for volume and permeability constraints. Graphical representation of anisotropy and parameter  $\mathcal{A}$ .

Macroscopic stresses	Volume constraint $V^* = 50\%$		Permeability constraint $k^* = 50\%$	
 $(\sigma_{11}; \sigma_{22}; \sigma_{33}; \sigma_{12}; \sigma_{23}; \sigma_{13})$	Topology	Anisotropy	Topology	Anisotropy
<b>Hydrostatic</b>  $(\sigma; \sigma; \sigma; 0; 0; 0)$		$\mathcal{A} = 0.1644$ 		$\mathcal{A} = 0.4351$ 
<b>Shear</b>  $(0; 0; 0; \sigma; 2\sigma; 1.5\sigma)$		$\mathcal{A} = 0.4200$ 		$\mathcal{A} = 0.3790$ 

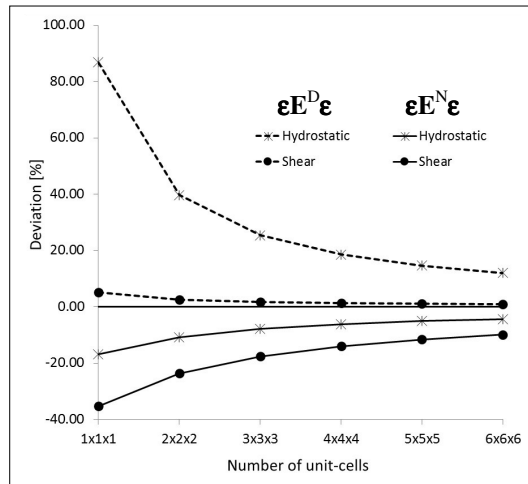


Figure 3: Strain energy density convergence for Dirichlet-type BC's and Neumann-type BC's.

The convergence of the strain energy density and the independent coefficients of the stiffness tensor to the homogenization values for the hydrostatic (with permeability) and shear (with volume constraint) cases are shown in Fig. 3 to 5, respectively. For the highest scale factor studied here ( $n = 6$ ), Fig. 3 shows a rapid rate of convergence of energy (deviations  $< 10\%$ ) and the longitudinal coefficient estimates  $E_{iii}^D$  and  $E_{iii}^N$  are below  $7\%$

of deviation with respect to homogenization (see Fig 4a, 4b and 5). However, estimates of  $E_{iii}^N$  are based on a moderate contrast ratio  $E^{\text{solid}}/E^{\text{void}} = 10$  rather than  $E^{\text{solid}}/E^{\text{void}} = 10^{12}$  used in the remaining cases. This avoids excessive compliance of the void phase making the Neumann BC's effective only for non-porous composites. To test porous materials, Neumann conditions can be slightly changed such that the uniform pressure is only applied on the solid phase or mixed BC's can be used also as explained in section 6. Having the analyses restricted to orthotropic cases, the resulting estimates deviate from homogenization less than 20%, as seen in Fig. 4c and 4d. In general, while the convergence of longitudinal coefficients is quite exceptional, the rate of convergence is not so good for some non-longitudinal coefficients. Enlarging the number of targeted tensor coefficients up to 21 with the shear case, one sees actually a pretty convergence in Fig. 5a with most deviations less than 10% for  $n = 6$ . Larger deviations are obtained in Fig. 5b.

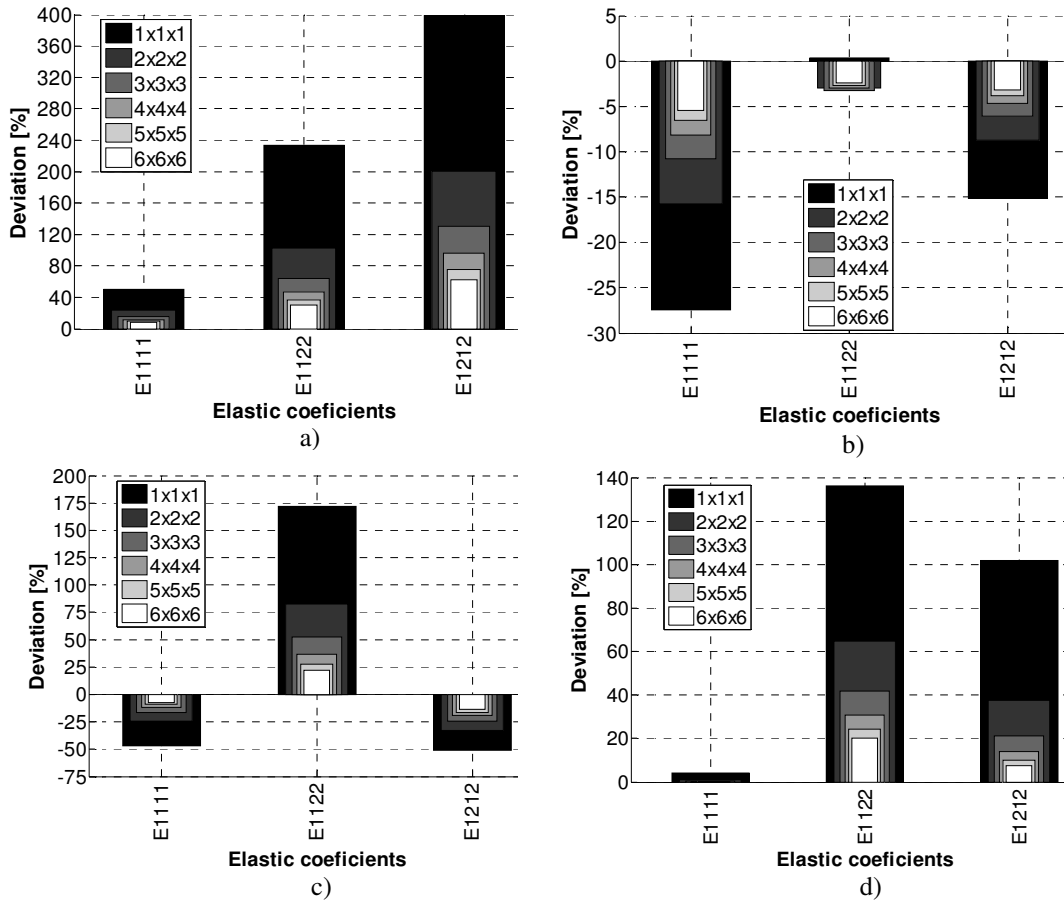


Figure 4: Scale-size effects analysis for the *hydrostatic* case. a) Dirichlet-type BC's; b) Neumann-type BC's with  $E^{\text{solid}}/E^{\text{void}} = 10$ ; c) Constant stress on solid; d) Mixed BC's.

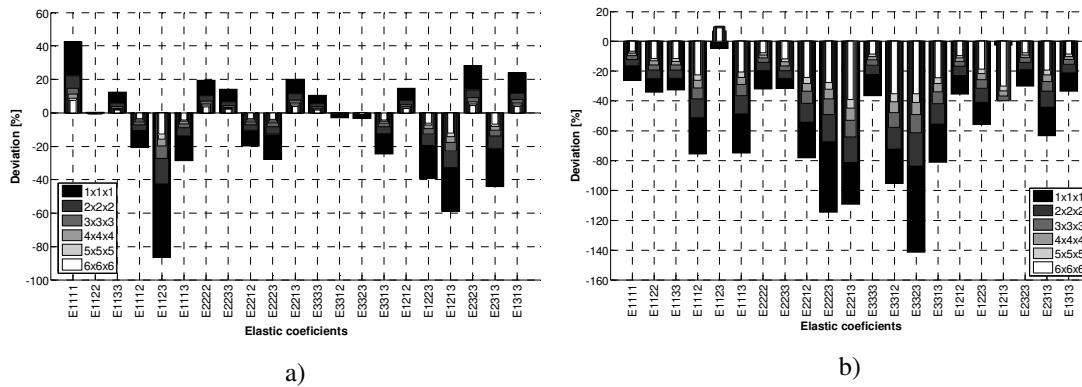


Figure 5: Scale-size effects analysis for the *Shear* case. a) Dirichlet-type BC's; b) Neumann-type BC's with  $E^{\text{solid}}/E^{\text{void}} = 10$ .

## 8. Conclusions

Homogenization assumes the unit-cell infinitely small and with periodic BC's. However, in practice, the composite material comprises a finite number of measurable unit-cells and the stress or strain fields are not periodic near the structure boundary. It is thus critical to investigate whether the obtained topologies are affected when applied in the context of real composites. This is done here by scaling the unit-cell an increasing number  $n$  of times. For each  $n$  one accesses the apparent properties of the resulting composite by means of numerical experiments applying *e.g.* Dirichlet and Neumann-type BC's. Alternative stress-based BC's are investigated to test porous materials overcoming excessive compliance of the void phase. Convergence to the homogenized properties can then be checked. The present work indicates that for practical purposes, even for microstructures with low scale factor ( $n = 6$ ), it is mechanically admissible to use the equivalent moduli given by the periodic homogenization theory.

## 9. References

- [1] J.E. Cadman, S. Zhou and Y. Chen, On design of multi-functional microstructural materials, *J Mater Sci*, 48:51-66, 2013.
- [2] M.P. Bendsøe and O. Sigmund, *Optimization. Theory, Methods and Applications*, Springer, 2003.
- [3] O. Sigmund, Materials with prescribed constitutive parameters: an inverse homogenization problem, *Int J Solid and Struct*, 31(7), 2313-2329, 1994.
- [4] P.G. Coelho, P.R. Fernandes and H.C. Rodrigues, Multiscale modeling of bone tissue with surface and permeability control, *Journal of Biomechanics*, 44(2), 321-329, 2011.
- [5] R.D. Marta, J.M. Guedes, C.L. Fanagan, S.J. Hollister and P.R. Fernandes, Optimization of scaffold design for bone tissue engineering: a computational and experimental study, *Journal Medical Engineering & Physics*, 36, 448-457, 2014.
- [6] J.K. Guest and J.H. Prévost, Optimizing multifunctional materials: design of microstructures for maximized stiffness and fluid permeability, *Int J of Solids and Struct*, 43, 7028-7047, 2006.
- [7] S.J. Hollister and Y.L. Cheng, Computational design of tissue engineering scaffolds, *Comput Methods Appl Mech Engrg*, 196, 2991-2998, 2007.
- [8] S. Xu and G. Cheng, Optimum material design of minimum structural compliance under seepage constraint, *Struct Multidisc Optim*, 41, 575-587, 2010.
- [9] H. Kang, C-Y. Lin and S.J. Hollister, Topology optimization of three-dimensional tissue engineering scaffold architectures for prescribed bulk modulus and diffusivity, *Struct Multidisc Optim*, 42, 633-644, 2010.
- [10] J.F. Bourgat, Numerical experiments of the homogenization method for operators with periodic coefficients, *Lecture Notes in Mathematics*, 704, 330-356, 1977.
- [11] A. Bensoussan, J.L. Lions and G. Papanicolaou, *Asymptotic analysis for periodic structures*, North-Holland, 1978.
- [12] E. Sanchez-Palencia, *Lecture Notes in Physics*, Vol 127, Springer-Verlag; 1980.
- [13] J.M. Guedes and N. Kikuchi, Preprocessing and postprocessing for materials based on the homogenization method with adaptive finite element method, *Comput Meth Appl Mech Eng*, 83, 143-198, 1990.
- [14] W. Zhang and S. Sun, Scale-related topology optimization of cellular materials and structures, *International Journal for Numerical Methods in Engineering*, 68, 993-1011, 2006.
- [15] G. Dai and W. Zhang, Cell size effects for vibration analysis and design of sandwich beams, *Acta Mech Sin*, 25, 353-365, 2009.
- [16] S. Pecullan, L.V. Gibiansky and S. Torquato, Scale effects on the elastic behavior of periodic and hierarchical two-dimensional composites, *Journal of the Mechanics and Physics of Solids*, 47, 1509-1542, 1999.
- [17] S.J. Hollister and N. Kikuchi, A comparison of homogenization and standard mechanics analyses for periodic porous composites, *Computational Mechanics*, 10, 73-95, 1992.
- [18] M.P. Bendsøe, Optimal shape design as a material distribution problem, *Structural Optimization*, 1, 193-202, 1989.
- [19] M.R. Dias, J.M. Guedes, C.L. Flanagan, S.J. Hollister and P.R. Fernandes, Optimization of scaffold design for bone tissue engineering: A computational and experimental study, *Med Eng Phys*, 36(4), 448-57, 2014.
- [20] P.G. Coelho, P.R. Fernandes and H.C. Rodrigues, Multiscale modeling of bone tissue with surface and permeability control, *Journal of Biomechanics*, 44(2), 321-329, 2011.
- [21] T.I. Zohdi and P. Wriggers, *Introduction to computational micromechanics*, Springer, 2004.
- [22] T. Böhlke and C. Brüggemann, Graphical representation of the generalized Hooke's Law, *Technische Mechanik*, 21, 145-158, 2001.
- [23] V.J. Challis, A.P. Roberts and A.H. Wilkins, Design of three dimensional isotropic microstructures for maximized stiffness and conductivity, *Int J Solids and Structures*, 45, 4130-4146, 2008.